Fractal Characterization of Wear-Erosion Surfaces

J. Rawers and J. Tylczak

(Submitted 9 June 1999; in revised form 18 August 1999)

Wear erosion is a complex phenomenon resulting in highly distorted and deformed surface morphologies. Most wear surface features have been described only qualitatively. In this study wear surfaces features were quantified using fractal analysis. The ability to assign numerical values to wear-erosion surfaces makes possible mathematical expressions that will enable wear mechanisms to be predicted and understood. Surface characterization came from wear-erosion experiments that included varying the erosive materials, the impact velocity, and the impact angle. Seven fractal analytical techniques were applied to micrograph images of wear-erosion surfaces. Fourier analysis was the most promising. Fractal values obtained were consistent with visual observations and provided a unique wear-erosion parameter unrelated to wear rate.

Keywords alumina, analysis, erosion, fractal, silicon carbide, tribology, wear

1. Introduction

Wear is characterized by material deterioration, which is a function of the materials involved and the processing environment. Wear can be characterized by the rate of material loss, wear mechanism, and wear surface features. Most wear parameters, or variables, can be quantified, for example, hardness, wear rate, and impact velocity. However, descriptions of wear mechanisms and of wear surfaces are generally based upon visual examination and the use of qualitative descriptive terms, such as impact, pitting, seizing, galling, scratching, grinding, gouging, and plowing. In this study, wear-erosion surfaces were quantified by assigning a fractal value to their micrographic features.

Wear erosion is caused by particles (solid or liquid) impacting a surface and the resulting surface material deterioration. The process is complex because complete knowledge of individual impacting particles and the impacted surface as a function of time is not known and generally cannot be known. During wear erosion, individual eroding particles generally have different shapes, speeds, masses, and angles of impact. As a result of varying particle morphologies and energies, and of random spatial and temporal nature of the impacts, the exact predictions of wear erosion based upon individual particle impacts may not be possible. Differences in individual impact-surface interactions also arise because most surfaces are composed of regions with different grain sizes, lattice grain orientations, and often different phases with different hardnesses. With successive impacts, new wear phenomenon emerge that are uniquely characteristic of collective impact deterioration, which requires a new level of wear-erosion understanding. For example, the first impacting particle may cause the surface to fragment, crack, and/or plastically deform. The material underneath the impact area work hardens and develops complex spatial tensile-compression relationships. Subsequent particle impacts to this region strike an undulating, deformed surface with varying degrees of surface damage, stresses, and hardness. After multiple impacts, the surface assumes an ensemble average wear rate and a global microstructure that can be characterized, but the surface has locally inhomogeneous structures with local wear characteristics that are impossible to predict. Thus, a set of collective phenomena that can be characterized and allow mass loss predictions and wear mechanisms to be generated emerge (Ref 1-5).

Previous students of wear have qualitatively described a variety of wear mechanisms and characterized the appearance of the resulting surfaces (Ref 1-5). Recently, there have been several attempts to use fractal analysis to quantitatively describe wear features and irregular material surfaces (Ref 6-9). Fractal analysis is a technique that has successfully been used to characterize fracture surfaces (Ref 10-12), surface roughness (Ref 9, 13, 14, 15), and wear debris (Ref 16, 17). Currently there is no surface measuring test that ascertained which wear mechanism generated a particular wear surface morphology, nor is there a quantitative procedure for measuring the surface morphology. This study describes a means of assigning a quantitative characterization to the wear-erosion surface morphology with the ultimate goal of relating this numerical characterization to wear-erosion mechanisms that might eventually lead to the ability to predict the wear mechanism from a particular set of parameters.

Most wear surface descriptions are obtained from two-dimensional, optical surface examinations. In this study, micrographic images of wear-erosion surfaces were analyzed. Quantitative characterization was accomplished by determining fractal values for the wear-erosion surface image using seven different analytical techniques. In a previous study to characterize wear-erosion surfaces using fractal analysis (Ref 7), a single technique for measuring the fractal dimension was successfully used. Although several areas of each sample were measured, the role of surface magnification was ignored. In addition to comparing different analytical techniques, this study expanded upon the results of the previous study. Wear erosion of stainless steel surfaces was studied as a function of different processing conditions including varying (a) impact angle, (b) impact velocity, and (c) erosive material. The surface morphology was

J. Rawers and J. Tylczak, U.S. Department of Energy, Albany Research Center, Albany, Oregon 97321. Contact e-mail: rawers@alrc.doe.gov.

fitted to a fractal value using different measuring schemes and different magnifications in order to characterize the same surface.

2. Erosion Wear

Reference 18 provides descriptions of the apparatus used to conduct the erosion-wear tests. Samples for impacting were sheets of 316 stainless steel 2 mm thick and 20 by 30 mm in length. Two erosive materials were used: 50 μm diameter Al_2O_3 and 120 μm SiC (Fig. 1). Erosive particles were entrained in a stream of inert gas and struck the stainless steel plate at two velocities: 40 m/s and 140 m/s. Two impact angles were used: 90 and 30°. Each experiment ran at room temperature for 20 min, delivering approximately 2 g of powder per minute (Fig. 2). Previous studies have shown that under these experimental conditions, additional processing time produced no significant change in wear-erosion global characteristics: wear rate and surface features. Multiple samples were run under experimentally identical conditions. After each test, the samples were weighed to determine material weight loss.

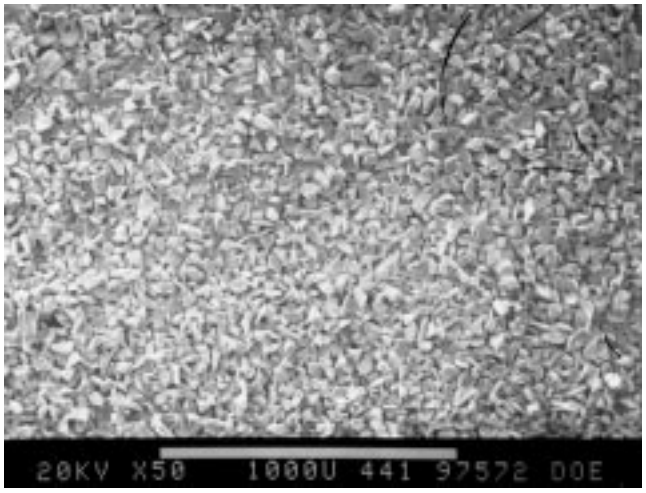

Fig. 1 Scanning electron micrograph of the Al_2O_3 erosive particles

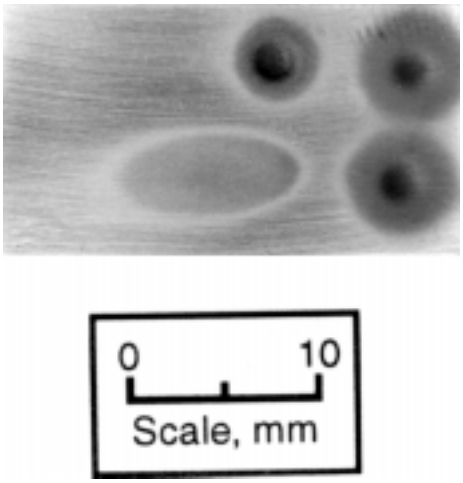

Fig. 2 Picture of wear sample after Al_2O_3 erosion test. Top left: 40 m/s, 90° impact angle. Bottom left: 40 m/s, 30° impact angle. Top and bottom right: duplicate runs, 40 m/s, 90° impact angle

Erosion-wear surfaces were then photographed using scanning electron microscopy (SEM) at different magnifications and in different wear areas. For two samples, images were scanned into a computer, and additional magnified images were generated. After the wear-erosion surface textures were quantified and assigned a fractal value, the samples were cross sectioned (Fig. 3). Fractal characterizations of the erosion-wear surface and cross-section profile micrographs were determined using computer analysis programs (Ref 6).

3. Surface Morphology Measurement

Fractals have been used to generate extremely complex and irregular surfaces, for example, clouds, trees, and artificial worlds, as in *Star Wars* movies (Ref 19). Fractal analysis has been used to describe complex physical phenomena such as turbulence, metastable systems, alternating current (ac) response, and 1/*f* noise (Ref 20). Fractal characterizations have also been used to describe complex two- and three-dimensional surfaces such as paint pigments, crushed ores, failure surfaces, and membranes (Ref 6, 21). Of particular importance in this study, fractal characterization has been shown to be used to assign a numerical value to inhomogeneous surfaces (Ref 6, 10-15).

A fractal dimension is the signature, characterization, or measure of the emergence of complexity in a system controlled by chaos or chaotic processes (Ref 22-26). With respect to wear erosion, emergence is the development of new phenomena or higher levels of organization from less complicated systems (e.g., the change in wear from that of a single particle impact to the cumulative effects of multiple impacts). Complexity is the set of rules or laws, generally in the form of nonlinear equations that characterize features of a system (e.g., the work hardening of the surface due to particle impacting). Chaos is the spread or variation in the measurement or in the predictability of a measurable parameter in a given system related to a common attractor (i.e., the inability to completely characterize the impact surface after repeated impacts, even after equilibrium or steady state conditions have been established). Fractal dimension is a numerical characterization for the new set of evolved parameters (i.e., the spatial characterization of the wear-erosion surface morphology).

In this study, fractal values of the erosion-wear surface images were obtained from SEM micrographs (Fig. 3). The numerical characterizations were a measure of the morphology, texture, and/or roughness in the surface images. The variation in the surface features, that is, changes in the gray scale of the micrograph, is the result of changes in surface roughness, elevation, and/or surface tilt. Because fractals determined in this study are not measures of spatial dimensions but rather of variation in structure, or more properly, variations in the gray scale of micrographs, fractals determined from the micrograph will be referred to as fractal values.

Seven fractal surface determination techniques were employed: dimension, Fourier, Kolmogorov, Korcak, Minkowski, root mean square (rms), and slit island (Fig. 4a-f) (Table 1). Description, applicability, and limitations of each technique are described by Russ in Ref 6. (A computer disk with the individual fractal analysis programs used in this study is supplied with the reference.)

4. Data and Analysis

Table 1 presents wear erosion results from six different wear erosion tests. Data include (a) surface fractal values determined from seven different analytical techniques as a function of processing parameters (impact velocity, impact angle, erosive material, and micrograph magnification), (b) weight loss, and (c) cross-section fractal value.

There was little or no correlation between the fractal analyses for cross section and surfaces; what correlation existed was negative, confirming the wear surface to be self affine. Self affine in this article describes a system where the fractal characterization in the different spatial dimensions or directions may be fractal, but each direction may have its own scale or fractal value. Figure 3 shows that the scale of wear-erosion damage out of the surface is different from the scale of damage across or along the surface.

Scanning electron microscopy micrographs of the different wear surfaces when viewed under similar magnifications show significant differences in surface texture, roughness, and/or morphology (Fig. 3). Surface roughness appears to decrease with increasing impact velocity and with increasing particle erodent size. However, the weight loss increases with increasing impact velocity and decreases with increasing particle size. Little or no correlation exists between surface fractal value and cross-section fractal value, weight loss, or processing parameters: velocity, angle, and erosive material (Table 2). Thus, the surface fractal value is a unique measure or characterization of the erosion-wear surface morphology, and thus, may be a unique, quantitative measure of the wear-erosive mechanism.

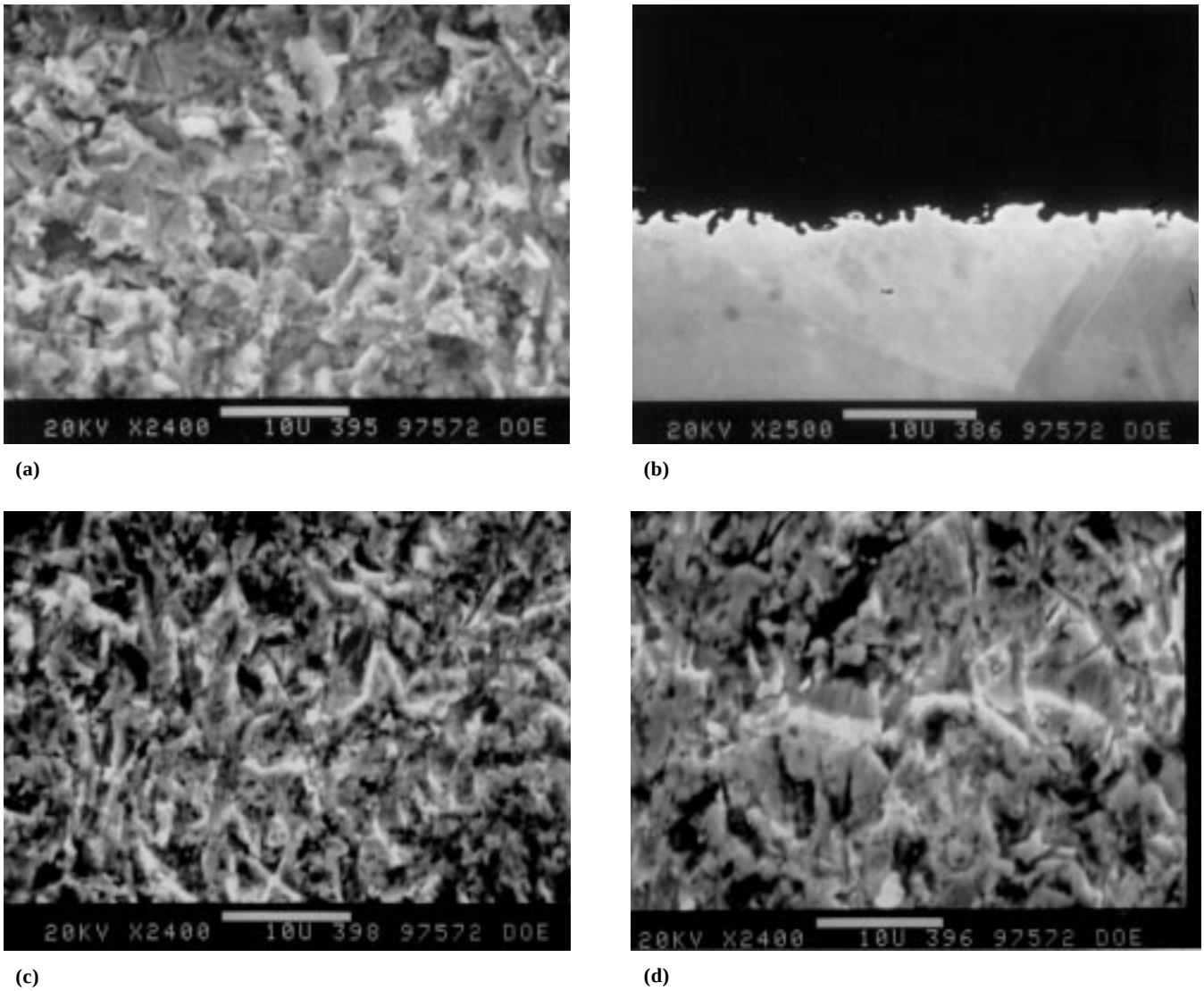

Fig. 3 Scanning electron micrographs for 50 μ Al_2O_3 erodent. (a) 90° high velocity surface. (b) Cross section. (c) 90° low velocity. (d) 30° low velocity

Table 1 Fractal value for the different wear-erosion experiments for the different surface fractal analytical techniques, the wear loss, and the fractal determined from the cross-section micrograph

Experiment	Minkowski	Kolmogorov	Korcak	Dimension	Slit island, 50%	Root mean square	Fourier	Weight loss, g	Cross section, ~5000×
50 μ Al_2O_3, 20 min, 90°, 40 m/s									
500	2.69 ± 0.04	2.95 ± 0.07	2.57 ± 0.03	2.97 ± 0.01	2.48 ± 0.09	2.475 ± 0.002	2.76 ± 0.05	0.00244	1.19 ± 0.02
1000	2.51 ± 0.04	2.84 ± 0.09	2.29 ± 0.05	2.83 ± 0.01	2.38 ± 0.09	2.442 ± 0.005	2.61 ± 0.05		
2600	2.23 ± 0.03	2.72 ± 0.09	2.04 ± 0.02	2.51 ± 0.01	2.27 ± 0.07	2.327 ± 0.007	2.32 ± 0.03		
50 μ Al_2O_3, 20 min, 90°, 40 m/s									
2000	2.41 ± 0.05	2.79 ± 0.10	2.22 ± 0.03	2.68 ± 0.01	2.60 ± 0.09	2.357 ± 0.006	2.42 ± 0.04	0.00241	1.14 ± 0.01
2000++	2.16 ± 0.04	2.67 ± 0.11	2.04 ± 0.03	2.45 ± 0.02	2.36 ± 0.09	2.271 ± 0.009	2.16 ± 0.02		
50 μ Al_2O_3, 20 min, 90°, 140 m/s									
500	2.43 ± 0.04	2.86 ± 0.11	2.25 ± 0.02	2.83 ± 0.02	2.48 ± 0.08	2.399 ± 0.007	2.57 ± 0.05	0.00495	1.27 ± 0.01
1000	2.38 ± 0.04	2.75 ± 0.09	2.14 ± 0.02	2.76 ± 0.02	2.37 ± 0.09	2.398 ± 0.006	2.48 ± 0.05		
2500	2.15 ± 0.03	2.56 ± 0.11	2.06 ± 0.04	2.44 ± 0.01	2.22 ± 0.06	2.280 ± 0.005	2.20 ± 0.04		
50 μ Al_2O_3, 20 min, 90°, 140 m/s									
2000	2.27 ± 0.04	2.69 ± 0.09	2.23 ± 0.04	2.57 ± 0.02	2.84 ± 0.06	2.324 ± 0.007	2.39 ± 0.04	0.00503	1.24 ± 0.01
2000+	2.24 ± 0.04	2.68 ± 0.10	2.19 ± 0.03	2.51 ± 0.02	2.72 ± 0.08	2.294 ± 0.005	2.15 ± 0.02		
2000++	2.10 ± 0.04	2.58 ± 0.11	2.14 ± 0.03	2.39 ± 0.02	2.47 ± 0.09	2.239 ± 0.008	2.10 ± 0.02		
50 μ Al_2O_3, 20 min, 30°, 40 m/s									
2000	2.31 ± 0.04	2.86 ± 0.08	2.61 ± 0.02	2.58 ± 0.01	2.65 ± 0.08	2.327 ± 0.007	2.34 ± 0.15	0.00288	1.11 ± 0.01
2000+	2.17 ± 0.04	2.67 ± 0.11	2.43 ± 0.03	2.52 ± 0.02	2.60 ± 0.08	2.293 ± 0.008	2.18 ± 0.13		
2000++	2.08 ± 0.04	2.59 ± 0.12	2.11 ± 0.04	2.33 ± 0.02	2.36 ± 0.08	2.218 ± 0.010	2.07 ± 0.11		
120 μ SiO_2, 90°, 40 m/s									
250	2.66 ± 0.04	2.93 ± 0.08	2.72 ± 0.03	2.88 ± 0.01	2.89 ± 0.07	2.459 ± 0.003	2.70 ± 0.05	0.00013	
470	2.49 ± 0.04	2.91 ± 0.06	2.69 ± 0.04	2.84 ± 0.01	2.73 ± 0.08	2.424 ± 0.004	2.57 ± 0.04		
1000	2.24 ± 0.04	2.75 ± 0.10	2.51 ± 0.02	2.75 ± 0.01	2.59 ± 0.08	2.376 ± 0.004	2.42 ± 0.04		

Table 2 Correlation between the Fourier fractal surface and cross-section values, the weight loss, and impact velocity

Parameters	Fourier fractal	Cross-section fractal	Weight loss, gms
Fourier	1.000	…	…
Cross section	0.003	1.000	…
Weight loss	–0.165	–0.154	1.000
Velocity	0.370	–0.520	0.990
Angle	–0.098	–0.222	0.322

For a given wear-erosion sample, fractal values from the different measuring techniques were dissimilar. However, a strong correlation existed between the relative ranking of fractal values obtained from the different fractal measuring techniques (Table 3). Similar results have been obtained between different fractal analytical techniques when applied to analysis of computer generated surfaces (Ref 6). Because of this high correlation, it is not necessary to discuss the results of each fractal analysis technique separately. The Fourier technique was chosen to represent surface fractal characterization because, in addition to providing an overall or average surface fractal value, the Fourier analytical technique provides fractal information as a function of surface orientation and the intercept of the log (magnitude) versus log (frequency) has also been interpreted and correlated with surface roughness (Ref 6). The data available in this limited study indicated a strong statistical correlation between the change in surface fractal value and the change in Fourier intercept, that is, surface roughness. However, until further experiments are conducted this conclusion remains suggestive but unproven.

Wear-erosion surfaces are self affine, arising from the difference in the scale of surface area features and the cross-section profile features. These variations are expected to produce different fractal values for different micrograph surface image magnifications (Ref 6). For a given wear-eroded surface, the variation in fractal values scaled with magnification and could be fitted to a linear equation:

$$F = F_o + \alpha^* \text{ magnification}$$

where F is the measured fractal value, F_o, is the constant fractal value for zero magnification, and α is the fractal magnification factor.

For a specific erosion-wear experiment, a high linear correlation existed between the measured fractal value and the magnification of the micrograph (greater than $R^2 = 0.95^+$). Physics of the experiment would suggest that the range of fractal characterization is limited by the size and morphology of the erosive material (Ref 21). The structure of the surface features is limited to less than 10 to 20× the size of the erosive particles. The texture of the surface is reflective of the flat faces of the erosive particles. The negative value for α (Table 4) is consistent with the higher magnification images reflecting more area of smooth imprint left by the impacting particle flat faces (Fig. 1).

For a given set of experimental conditions, this fractal-magnification scale correlation was valid for different surfaces prepared under similar experimental conditions, different SEM magnifications, or different computer enhanced magnified images. However, for surfaces prepared under different

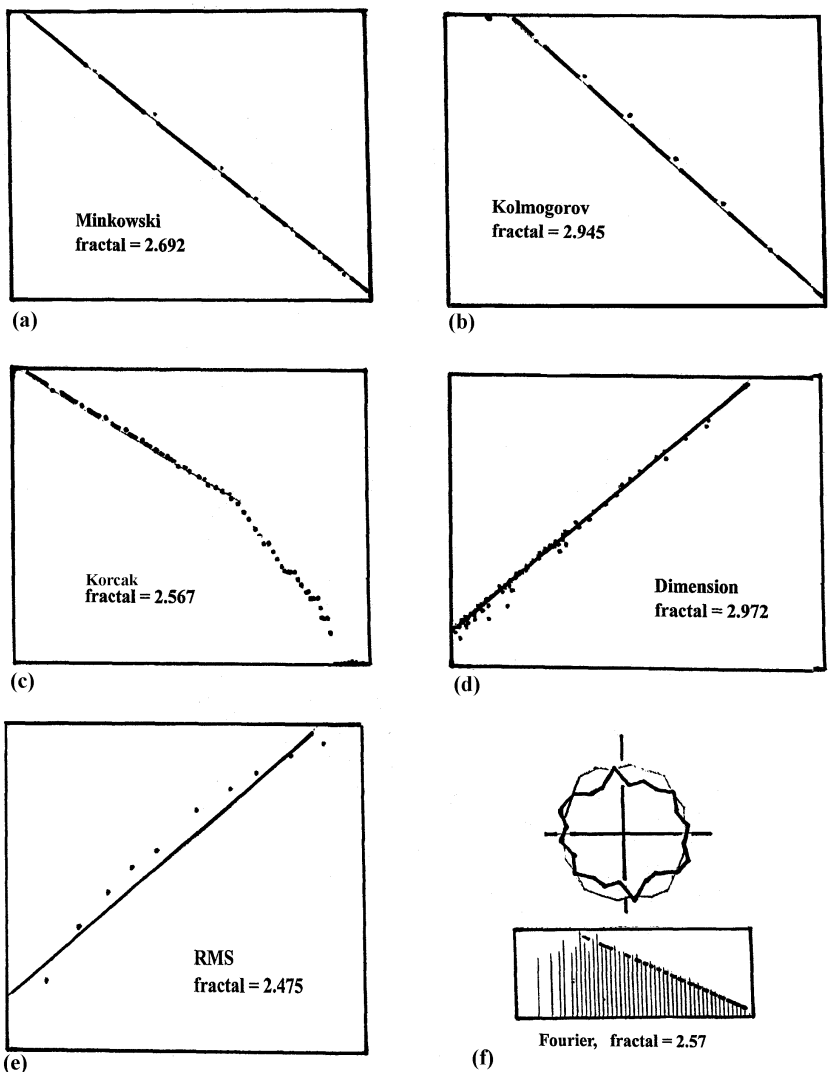

Fig. 4 Fractal fit 470 magnification images for 50 μ Al_2O_3 erodent 90° impact angle, 40 m/s. The fractal value is determined by a fitting of the data points to a straight line. Units and axes descriptions have not been included but can be found along with interpretation and derivation of the fractal dimension in Ref 6. (a) Minkowski. (b) Kolmogorov. (c) Korcak. (d) Dimension. (e) Root mean square. (f) Fourier

Table 3 Correlation table for the different fractal values determined by the seven analytical techniques in this study for the Al_2O_3 erodent, 90° impact angle, and 14 m/s

Experiment	Kolmogorov	Dimension	Minkowski	Root mean square	Korcak	Slit island	Fourier	Magnification
Kolmogorov	1.000	…	…	…	…	…	…	…
Dimension	0.987	1.000	…	…	…	…	…	…
Minkowski	0.951	0.988	1.000	…	…	…	…	…
Root mean square	0.912	0.966	0.994	1.000	…	…	…	…
Korcak	0.999	0.991	0.961	0.924	1.000	…	…	…
Slit island	0.964	0.994	0.999	0.979	0.973	1.000	…	…
Fourier	0.928	0.975	0.999	0.999	0.939	0.993	1.000	…
Magnification	–0.982	–0.999	–0.992	–0.972	–0.988	–0.996	–0.981	1.000

wear-erodent conditions, the fractal magnification function, α, changed (Table 4). This relationship between α and magnification is consistent with wear surfaces being self affine. As stated previously, preliminary examination of the Fourier fractal analysis shows the intercept value to be related to surface roughness and α.

Variation in fractal values is also anticipated for surfaces that have different erodent impacting angles. The 90° impinging particles made spherical impact, whereas the 30° impinging particles made directional, glancing, or elongated impacts. Fourier analysis also provides fractal value information as a function of orientation (Fig. 5a and b). Note that the

180° symmetry is due to the symmetry of the trigonometric functions used in the Fourier analysis. Variation in fractal value for the 90° impact erodents is minimal and is essentially independent of orientation around the wear surface. However, there is a significant directional variation in the fractal value around the surface for the 30° impact erodents. In addition to this directional fractal value information (heavy line), the figures also include the Fourier intercept value, which is thought to contain information about surface roughness (thin line). For the 30° impact experiment, the lower the Fourier intercept value is associated with the direction of impact, as anticipated for a glancing impact. As previously mentioned, the intercept data provides information consistent with visual examination of the wear surface. This observation is quantitatively supported by the strong correlation between the Fourier intercept value and fractal dimension, regardless of the erodent, impact angle, impact velocity, and image magnification (Fig. 6). However, more study needs be conducted before this intercept data can be correlated and interpreted with wear erosion.

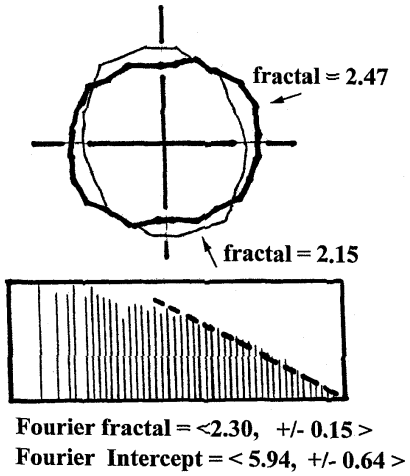

(a)

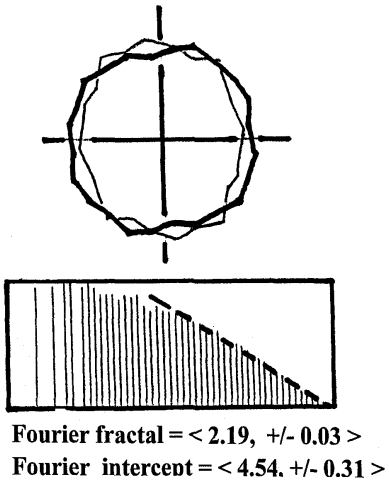

(b)

Fig. 5 Fractal Fourier plots and fractal and intercept values for 40 m/s. The 50 μ Al_2O_3 erosive particles wear surfaces for (a) 30° and (b) 90° impact angles

5. Discussion

Due to the complex nature of wear erosion even for the most carefully controlled experiments, it is impossible to duplicate all the wear-erodent surface interactions and thus to have identical results, for example, identical weight loss and identical wear surface morphology. However, the complexity of the individual events does not mean that it is impossible to develop an understanding of the collective events. Because of the complexity of the wear-erosion phenomenon, a reductionist approach of explaining wear erosion from an understanding of individual impacts may not be practical; instead, perhaps a better approach to understanding wear erosion would be to study the emergence of new wear-erosion phenomena such as surface morphology, wear rate, and so on.

This study was designed to quantify one wear-erosion emergent feature, surface morphology resulting from collective impacts, by fractal characterization. Wear-erosion surfaces were made on the same material using several different experimental conditions: different impact velocities, different erodents, and different impact angles. Visual examination of the surfaces showed significant differences in the surface features among the various processing environments. The visual trends were consistent and easily correlated with the measured fractal value

Table 4 Determination of the fractal magnification factor for the differnt fractal analytical techniques

$F = F_0 + \alpha^*$ magnification	Al_2O_3 (90°, 40 m/s)	Al_2O_3 (90°, 140 m/s)	SiC (90°, 40 m/s)
Minkowsky	–0.00022	–0.00014	–0.00045
Kolmogorov	–0.00011	–0.00015	–0.00023
Korack	–0.00024	–0.00008	–0.00026
Dimension	–0.00023	–0.00020	–0.00017
Slit island	–0.00010	–0.00012	–0.00029
Root mean square	–0.00008	–0.00022	–0.00009
Fourier	–0.00021	–0.00018	–0.00029

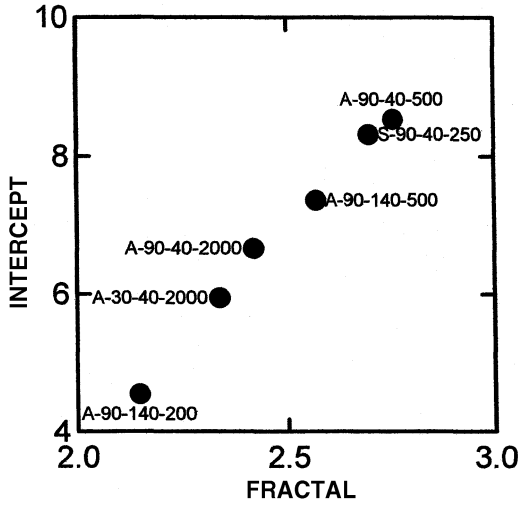

Fig. 6 Plot of Fourier intercept versus fractal value. Sample identification (*w-x-y-z*): *w*, erosive particle (A, Al_2O_3; S, SiC, impact angle); *x*, impact angle; *y*, impact velocity (m/s); *z*, micrograph magnification

trends. Thus, the results of this study strongly suggest that the wear-erosion surface is fractal and that the micrographs of these surfaces can be assigned a quantitative fractal value.

The findings of this study are consistent with previous findings (Ref 6, 7) with respect to correlations and trends between surface fractal values and (a) different erosive materials, (b) different velocities, (c) measured wear rates (Table 5), and (d) different fractal analytical techniques.

This study showed there was a linear relationship between magnification of the surface features and fractal value for a given wear-erosion surface regardless of what analytical technique was used or how that magnification was obtained by optical or computer enhancement. This relationship was unique to each wear erosion surface morphology generated under identical experimental conditions. Variation in the magnification factor is a current limitation on the applicability of fractal analysis for surface characterization. In this respect, the role that self affinity and its correlated and quantified effects on image magnification has on the fractal value needs to be investigated. However, this study showed a relationship between the Fourier surface roughness parameter and magnification factor, which suggested that, with further research, this sample-magnification limitation might be understood and overcome.

Table 5 Comparison between results in this study and previous wear-erosion surface fractal analysis

Values	Reference 7		This study	
Velocity	40 m/s	90 m/s	40 m/s	140 m/s
Wear rate	0.71×10^{-4}	11.75×10^{-4}	24.4×10^{-4}	49.5×10^{-4}
Fractal value	2.350	2.305	2.84 (2.68)	2.75 (2.48)
Erodent	Al_2O_3	SiC	Al_2O_3	SiC
Wear rate	2.08×10^{-4}	11.75×10^{-4}	24.4×10^{-4}	1.3×10^{-4}
Fractal value	2.302	2.305	2.84 (2.68)	2.75 (2.42)

Values in this table are Kologorov fractals values used in both studies. Values in parentheses, (xx), are Fourier data.

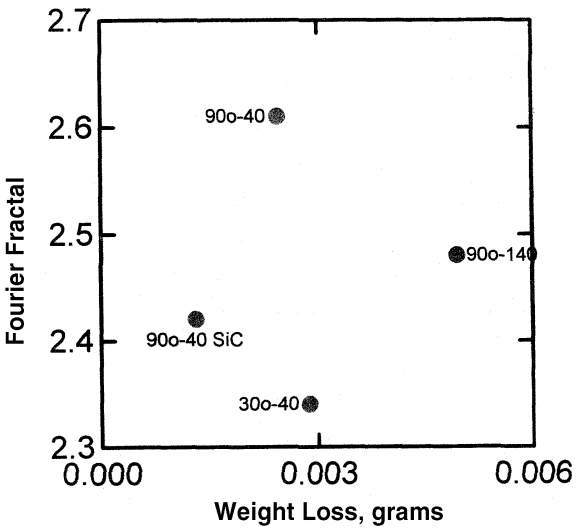

Fig. 7 Plot of Fourier fractal value versus wear rate. Sample identification (*x*-y) *x* = angle of impact, *y* = impact velocity. All data points are for Al_2O_3 except for data point marked SiC.

Fractal characterization values for the surface were dependent on the analytical method used to generate the fractal value. Comparison of the different fractal analysis methods showed a strong correlation in the ranking of the fractal between analytical techniques. There is every reason to believe that further investigations will be able to develop physical explanations and to derive mathematical expressions that will enable different fractal techniques to be correlated.

This study shows that fractal analysis and comparison is valid between wear erosion surface images if the images are all at the same magnification and the same fractal analytical technique is used. While each of the analytical techniques used in this study provided a fractal value consistent with visual observation, the most promising fractal analytical technique is Fourier analysis, which provides not only a global fractal characterization value, but also insight into angular variation in surface feature and surface roughness. The two Fourier numerical values, fractal value and intercept, and the additional orientation information for a wear erosion surface provide a better characterization of a multidimensional surface than does the single fractal value provided by other techniques.

6. Conclusions

This study on wear erosion showed that surface morphology could be quantified using fractal analysis. The fractal values obtained from wear-erosion micrographs are not necessarily a spatial dimension measure, but are related to wear-erosion space, that is, surface texture, roughness, or morphology and possibly related to wear-erosion mechanisms. The measured wear space fractal is self affine and thus highly dependent upon the measuring techniques that can be accounted for and incorporated in the analysis. The resulting fractal value is also a function of the technique used to analyze the surface (that is, Fourier, Kologorov, etc.).

When the proper correlations are met (the same analytical technique and possibly the same image magnification), the resulting fractal values provide a unique measure of the erosion-wear surfaces. Qualitative descriptions made from visual examinations of the erosion-wear surface are readily correlated to the measured fractal value. For example, the "rougher" the texture the higher the fractal number. Of equal importance, the measured fractal value is a unique wear space parameter not related to weight loss (Fig. 7). Thus, the surface fractal value provides another quantifiable parameter that can be used to understand and characterize erosion wear.

References

1. I. Hutchings, *Tribology: Friction and Wear of Engineering Materials*, CRC Press, 1992
2. K. Ludema, *Friction, Wear, Lubrication*, CRC Press, 1996
3. A. Sarkar, *Wear of Metals*, Pergamon Press Inc., 1976
4. E. Rabinowicz, *Friction and Wear of Materials*, John Wiley & Sons, Inc., 1995
5. A. Levy, *Solid Particle Erosion and Erosion-Corrosion of Materials*, ASM International
6. J. Russ, *Fractal Surfaces*, Plenum Press, 1994
7. S. Srinivasan, J. Russ, and R. Scottergood, *J. Mater. Res.*, Vol 5 (No. 11), 1990, p 2616-2619

8. Z. Chen, J. Mecholsky, T. Joseph, and C. Beatty, *J. Mater. Sci.*, Vol 32 (No. 23), 1997, p 6317-6323
9. P. Stupak, J. Kang, and J. Donovan, *Wear,* Vol 141 (No. 1), 1990, p 73-84
10. J. Hsiung and T. Chow, *J. Mater. Sci.,* Vol 33 (No. 11), 1998, p 2949-2953
11. L. Richards and B. Dempsey, *Scr. Metall.,* Vol 22, 1988, p 687-689
12. L. Meisel, *J. Phys. D,* Vol 24 (No. 6), 1991, p 942-952
13. A. Majumdar and C. Tien, *J. Heat Transfer,* Vol 113, 1991, p 516-525
14. G. Zhou, M. Leu, and D. Blackmore, *Wear,* Vol 170, 1993, p 1-14
15. A. Majumdar and C. Tien, *Wear,* Vol 136 (No. 2), 1990, p 313-327
16. M. Zhang, L. Song, and H. Zeng, *Adv. Comp. Lett.,* Vol 5 (No. 5), 1996, p 137-141
17. M. Zhang, L. Song, H. Zung, and F. Freeidick, *J. Mater. Sci. Lett.*, Vol 15 (No. 15), 1996, p 1288-1290
18. D. Alman, J. Tylczak, J. Hawk, and M. Hebsur, *Mater. Sci. Eng. A.*, Vol 261, 1998, p 245-251
19. B. Mandelbrout, *Fractal Geometry of Nature,* W. Freeman & Co., New York, 1983
20. L. Pietronero and E. Tosatti, *Fractals in Physics,* North-Holland Co., New York, 1985
21. B. Kayes, *Random Walk through Fractal Dimensions,* VCH Publishing Inc., New York, 1989
22. G. Baker and J. Gollup, *Chaotic Dynamics,* Cambridge University Press, Cambridge, UK, 1990
23. M. Schwedon, *Fractal, Chaos, and Power Laws,* W.H. Freeman & Co., New York, 1990
24. M. Barnsely and S. Demko, *Chaotic Dynamics and Fractals,* Academic Press, New York, 1986
25. D. Ruelle, *Chaotic Evolution and Strange Attrictors,* Cambridge University Press, Cambridge, UK, 1990